AMERICAN SOCIETY FOR MICROBIOLOGY | Journal of Bacteriology®

RESEARCH ARTICLE

Interaction of *Mycoplasma hominis* PG21 with Human Dendritic Cells: Interleukin-23-Inducing Mycoplasmal Lipoproteins and Inflammasome Activation of the Cell

J. Goret,[a,b,c] L. Béven,[d] B. Faustin,[e] C. Contin-Bordes,[e] C. Le Roy,[a,b] S. Claverol,[f] H. Renaudin,[a,b,c] C. Bébéar,[a,b,c] S. Pereyre[a,b,c]

Univ. Bordeaux, USC EA 3671 Mycoplasmal and chlamydial infections in humans, Bordeaux, France[a]; INRA, USC EA 3671 Mycoplasmal and chlamydial infections in humans, Bordeaux, France[b]; Laboratoire de Bactériologie, CHU de Bordeaux, Bordeaux, France[c]; Univ. Bordeaux, INRA, UMR BFP, Villenave d'Ornon, France[d]; Univ. Bordeaux, CNRS, UMR 5164, Bordeaux, France[e]; Pôle Protéomique, Plateforme Génomique Fonctionnelle de Bordeaux, Univ. Bordeaux, Bordeaux, France[f]

ABSTRACT *Mycoplasma hominis* lacks a cell wall, and lipoproteins anchored to the extracellular side of the plasma membrane are in direct contact with the host components. A Triton X-114 extract of *M. hominis* enriched with lipoproteins was shown to stimulate the production of interleukin-23 (IL-23) by human dendritic cells (hDCs). The inflammasome activation of the host cell has never been reported upon *M. hominis* infection. We studied here the interaction between *M. hominis* PG21 and hDCs by analyzing both the inflammation-inducing mycoplasmal lipoproteins and the inflammasome activation of the host cell. IL-23-inducing lipoproteins were determined using a sequential extraction strategy with two nondenaturing detergents, Sarkosyl and Triton X-114, followed by SDS-PAGE separation and mass spectrometry identification. The activation of the hDC inflammasome was assessed using PCR array and enzyme-linked immunosorbent assay (ELISA). We defined a list of 24 lipoproteins that could induce the secretion of IL-23 by hDCs, 5 with a molecular mass between 20 and 35 kDa and 19 with a molecular mass between 40 and 100 kDa. Among them, lipoprotein MHO_4720 was identified as potentially bioactive, and a synthetic lipopeptide corresponding to the N-terminal part of the lipoprotein was subsequently shown to induce IL-23 release by hDCs. Regarding the hDC innate immune response, inflammasome activation with caspase-dependent production of IL-1β was observed. After 24 h of coincubation of hDCs with *M. hominis*, downregulation of the NLRP3-encoding gene and of the adaptor PYCARD-encoding gene was noticed. Overall, this study provides insight into both protagonists of the interaction of *M. hominis* and hDCs.

IMPORTANCE *Mycoplasma hominis* is a human urogenital pathogen involved in gynecologic and opportunistic infections. *M. hominis* lacks a cell wall, and its membrane contains many lipoproteins that are anchored to the extracellular side of the plasma membrane. In the present study, we focused on the interaction between *M. hominis* and human dendritic cells and examined both sides of the interaction, the mycoplasmal lipoproteins involved in the activation of the host cell and the immune response of the cell. On the mycoplasmal side, we showed for the first time that *M. hominis* lipoproteins with high molecular mass were potentially bioactive. On the cell side, we reported an activation of the inflammasome, which is involved in the innate immune response.

KEYWORDS *Mycoplasma hominis*, human dendritic cells, lipoproteins, lipopeptide, inflammasome, PCR array, caspase, IL-1β, IL-23, interaction, innate response

Received 5 April 2017 **Accepted** 18 May 2017

Accepted manuscript posted online 30 May 2017

Citation Goret J, Béven L, Faustin B, Contin-Bordes C, Le Roy C, Claverol S, Renaudin H, Bébéar C, Pereyre S. 2017. Interaction of *Mycoplasma hominis* PG21 with human dendritic cells: interleukin-23-inducing mycoplasmal lipoproteins and inflammasome activation of the cell. J Bacteriol 199:e00213-17. https://doi.org/10.1128/JB.00213-17.

Editor Thomas J. Silhavy, Princeton University

Address correspondence to S. Pereyre, sabine.pereyre@u-bordeaux.fr.

Mycoplasmas are small bacteria that lack a cell wall. Their membranes contain a large number of lipoproteins that are anchored to the extracellular side of the plasma membrane, in direct contact with the host components. Many mycoplasmal lipoproteins have been reported to be involved in adhesion to host cells but also in the recognition by the host immune system (1). Indeed, mycoplasmal lipoproteins can act as proinflammatory factors and can stimulate human macrophages and human dendritic cells (hDCs), induce cytokine production, activate NF-κB, and polarize the adaptive immune response (2–8). Nondenaturing detergent extracts, such as Triton X-114 (TX-114) extracts enriched with mycoplasmal lipoproteins, were shown to have modulatory capacities (2, 5, 6, 9, 10). In addition, synthetic lipopeptides derived from lipoproteins such as MALP-2 from *Mycoplasma fermentans* (11), FSL-1 from *M. salivarium* (12), and MPPL-1 from *M. pneumoniae* (13) were shown to have immunomodulatory properties.

In *M. hominis*, which is a human urogenital pathogen involved in gynecologic and opportunistic infections, Peltier et al. partially purified from a TX-114 extract a macrophage-stimulating factor of 29 kDa that could stimulate tumor necrosis factor alpha (TNF-α) production by the THP-1 macrophage cell line (3). Recently, Hasebe et al. isolated and purified a lipoprotein of 40 kDa from an octyl-glucopyranoside (OG) extract derived from *M. hominis* membranes (14). This lipoprotein, which is a truncated form of the Vaa adhesin, also induced TNF-α production by the THP-1 cell line. Additionally, we showed that a TX-114 extract of *M. hominis* membranes induced the maturation of human dendritic cells (hDCs) and stimulated the production of proinflammatory cytokines such as interleukin-12 (IL-12) and TNF-α by hDCs (8). This *M. hominis* extract also induced a predominant IL-23 secretion that promoted the development of an IL-17-producing $CD4^+$ helper T cell subset and polarized the adaptive immune system toward the IL-23/Th-17 axis (8). Although inflammasome activation has not yet been reported in *M. hominis*, the activation of the NLRP3 and NLRP7 inflammasome has been described for other mycoplasmal species such as *M. pneumoniae*, *M. hyorhinis*, *M. salivarium*, and *Acholeplasma laidlawii* (15–18).

In the present study, to further examine both sides of the interaction between *M. hominis* and hDCs, we assessed (i) the *M. hominis* lipoproteins that could induce IL-23 production by hDCs using a sequential extraction strategy with two nondenaturing detergents and (ii) the activation of the hDC inflammasome using PCR array and enzyme-linked immunosorbent assay (ELISA).

RESULTS

Selective extraction of *M. hominis* lipoproteins that induce IL-23 production by hDCs. A simple TX-114 extract of *M. hominis* membranes contains a large number of proteins, including transmembrane proteins and lipoproteins (8). To obtain an *M. hominis* fraction enriched in bioactive lipoproteins, we developed a strategy based on the sequential use of two nondenaturing detergents. The goal here was to remove most nonbioactive proteins after the first extraction step and to selectively extract the bioactive molecules from the remaining fraction using TX-114. Five detergents were evaluated for their capacity to extract proteins from *M. hominis* membranes. Sarkosyl extracted a larger number of proteins than TX-100, OG, CHAPS {3-[(3-cholamidopropyl)-dimethylammonio]-1-propanesulfonate}, and deoxycholate (DOC) (see Fig. S2 in the supplemental material). Both Sarkosyl-insoluble fractions (IF_{Sar}) and Sarkosyl-soluble fractions (SF_{Sar}) were evaluated for their capacity to induce IL-23 production when added to hDCs. After 24 h of incubation, a significant IL-23 release was observed with the IF_{Sar} but not with SF_{Sar} (Fig. 1), indicating that the bioactive proteins were present in the IF_{Sar}.

A second round of extraction was undertaken by TX-114 partitioning applied to the IF_{Sar}. Upon electrophoretic separation, the IF_{Sar}-DP_{TX} sequential extract (i.e., Sarkosyl-insoluble fraction extracted by TX-114) showed fewer bands than a simple TX-114 extract (DP_{TX}) (see Fig. S3 in the supplemental material). These bands were also of higher intensity, suggesting an enrichment in specific proteins. To check whether the

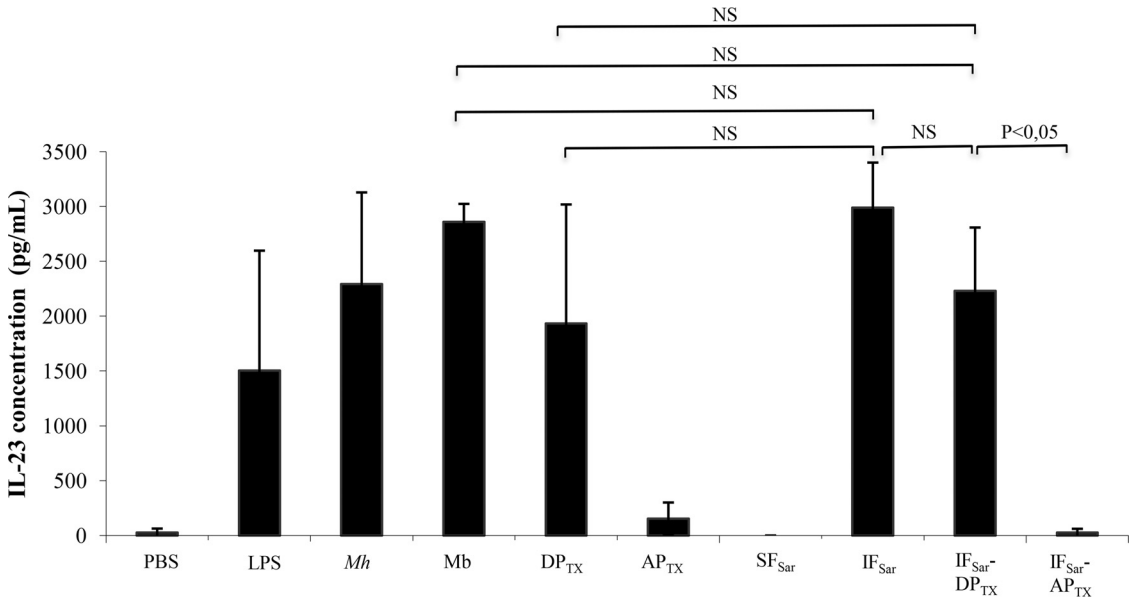

FIG 1 Release of IL-23 by hDCs after incubation with *M. hominis* PG21 and detergent extracts. hDCs were incubated 24 h at 37°C with the different detergent extracts. Supernatants were collected, and IL-23 concentration was determined by ELISA. Results are shown as the means and standard errors of the means from three independent experiments. PBS, negative control; LPS, positive control; *Mh*, *M. hominis* PG21; Mb, *M. hominis* PG21 membranes; DP_{TX}, Triton X-114 (TX-114) detergent phase (extracted proteins); AP_{TX}, TX-114 aqueous phase (nonextracted proteins); SF_{Sar}, Sarkosyl-soluble fraction (extracted proteins); IF_{Sar}, Sarkosyl-insoluble fraction (nonextracted proteins); IF_{Sar}-DP_{TX}, Sarkosyl-insoluble fraction extracted by TX-114 (detergent phase); IF_{Sar}-AP_{TX}, Sarkosyl-insoluble fraction extracted by TX-114 (aqueous phase); NS, statistically nonsignificant according to the Newman-Keuls test.

bioactive lipoproteins were recovered at the end of the sequential extraction procedure, IL-23 released by hDCs incubated for 24 h with IF_{Sar}-DP_{TX} was measured (Fig. 1). The IF_{Sar}-DP_{TX} sequential extract triggered a substantial release of IL-23, and the levels of IL-23 production were similar to those measured after incubation with *M. hominis* cells, with *M. hominis* membranes, or with the simple TX-114 extract (DP_{TX}).

Finally, the use of Sarkosyl as the initial detergent allowed the removal of many proteins without eliminating bioactive lipoproteins, validating the use of the sequential extraction procedure using Sarkosyl followed by TX-114 in further experiments.

Identification of the lipoproteins in the bioactive IF_{Sar}-DP_{TX} sequential extract. The IF_{Sar}-DP_{TX} sequential extract was further fractionated based on the protein molecular mass (MM). After electrophoretic separation, the gel slice was cut into 10 equal bands, from which proteins were extracted using OG in order to obtain 10 eluates, E1 (higher MM) to E10 (lower MM). The dendritic cell-activating potency of the eluates was evaluated by measuring the IL-23 release by hDCs incubated in the presence of each of the E1 to E10 fractions for 24 h (Fig. 2).

Five eluates (E3 to E5, E7, and E8) triggered the release of a significant amount of IL-23 by hDCs. The bioactive proteins present in eluates E3, E4, and E5 had a high apparent molecular mass (AMM), ranging from 40 to 100 kDa. The proteins in eluates E7 and E8 had a low AMM, from 20 to 35 kDa. No significant IL-23 release was observed for the E2 and E6 eluates. The bioactive compounds able to induce IL-23 release could correspond to two or more unrelated proteins or to different fragments of the same protein.

The lipoproteins from the bioactive eluates E3, E4, E5, E7, and E8 were identified by liquid chromatography-tandem mass spectrometry (LC-MS/MS) (Table 1). The E2 and E6 eluates that did not induce IL-23 production were also analyzed by LC-MS/MS as reference. Lipoproteins were considered nonfragmented when the AMM was close to that calculated on the basis of their predicted molecular mass. A total of 26 of the 48 *M. hominis* predicted lipoproteins (19, 20) were detected, i.e., 54.2% of the lipoproteins predicted *in silico* (Table 1). Two lipoproteins, MHO_1640 and MHO_3620, which were solely present in the E2 and E6 eluates, which did not induce IL-23 release from hDCs,

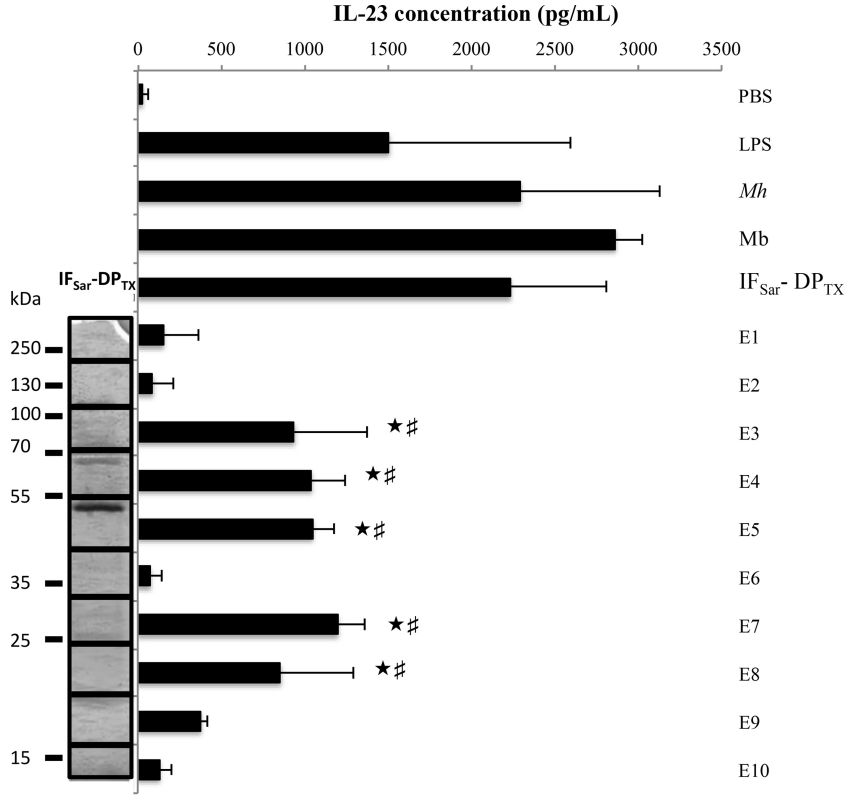

FIG 2 Release of IL-23 by hDCs after coincubation with the 10 eluates from the gel-separated sequential extract. Results are shown as the means and standard errors of the means from three independent experiments. PBS, negative control; LPS, positive control; *Mh*, *M. hominis* PG21; Mb, *M. hominis* PG21 membranes; IF_{Sar}-DP_{TX}, Sarkosyl-insoluble fraction treated by TX-114 (detergent phase). ★, significantly different ($P < 0.05$) from PBS according to the Newman-Keuls *post hoc* test; #, significantly different ($P < 0.05$) from IL-23 concentration released after coincubation with E2, E6, and E9 eluates according to the Newman-Keuls test.

were not considered to be bioactive. Vaa (MHO_3470) could not be considered inactive, although it was identified in the E2 and E6 eluates. Indeed, Vaa-derived peptides were recovered mainly in the bioactive E5 eluate, and either the entire Vaa or a Vaa-derived fragment with an AMM of >40 kDa could be responsible for the observed bioactivity in this eluate. Nonfragmented OppA (MHO_1510), Lmp1 (MHO_0530), and P120 (MHO_3660) proteins were also identified in the inactive E2 eluate. Consequently, the nonfragmented forms of these proteins could be considered inactive. However, for all three proteins, the fragmented forms detected in the E3 and E4 eluates could represent bioactive polypeptides.

MHO_4720 was the only unfragmented lipoprotein identified in the E8 eluate. Although we could not exclude the bioactivity of fragments of the other lipoproteins detected in the E8 eluate (MHO_3200, MHO_3470, MHO_3720), MHO_4720 could by itself be responsible for the bioactivity of E7 and E8 eluates.

Overall, 24 *M. hominis* lipoproteins (entire or degraded forms) were able to induce the secretion of IL-23 by hDCs, 5 with an AMM between 20 and 35 kDa and 19 with an AMM between 40 and 100 kDa (Table 1). In further experiments, more attention will be focused on MHO_4720, which may be the only bioactive protein in the E7 and E8 eluates.

Role of the polypeptidic portion of the lipoproteins in IL-23 production by hDCs. To assess whether *M. hominis* lipoprotein polypeptide fragments were responsible for the hDC stimulation, the IF_{Sar}-DP_{TX} sequential extract was incubated with proteinase K (PK) for 1 h (Fig. 3), and IL-23 release was measured after incubating hDCs in the presence of the PK-digested extract. The bioactivity of the PK-treated

TABLE 1 Lipoproteins identified by LC-MS/MS in eluates E2 to E8[a]

Gene locus	Product	No. of peptides identified in eluate:							Calculated MM (kDa)
		E2 (100–200 kDa)	E3 (70–100 kDa)	E4 (55–70 kDa)	E5 (40–55 kDa)	E6 (30–40 kDa)	E7 (25–30 kDa)	E8 (15–25 kDa)	
MHO_0280	Hypothetical protein, predicted lipoprotein		47	28	8	6			80.5
MHO_0290	Pseudogene of hypothetical protein (N-terminal part), predicted lipoprotein		55	21	11		2		67.7
MHO_0530	Lmp1 protein	13	5	2					170.7
MHO_0540	Lmp-related protein		3	28					70.0
MHO_0720	Conserved hypothetical protein, predicted lipoprotein		53	20					75.2
MHO_0730	Hypothetical protein, putative nuclease, predicted lipoprotein						2		34.3
MHO_0780	Conserved hypothetical protein, predicted lipoprotein		24	10					78.2
MHO_0790	Conserved hypothetical protein, predicted lipoprotein	5	61	27	13	2	2		78.2
MHO_1510	P100 = OppA, oligopeptide ABC transporter substrate-binding protein	44	36	24	7				105.8
MHO_1640[b]	Lmp3 protein	4							178.0
MHO_1730	Hypothetical protein, predicted lipoprotein						11		27.1
MHO_2080	Conserved hypothetical protein, predicted lipoprotein			8					64.3
MHO_2340	Hypothetical protein, putative adhesin, predicted lipoprotein			18					64.6
MHO_2440	Hypothetical protein, predicted lipoprotein					4	10		24.3
MHO_2620	Hypothetical protein, predicted lipoprotein			18	2				50.5
MHO_3070	Lmp related protein				24				44.2
MHO_3100	P75 related protein, predicted lipoprotein			39					62.3
MHO_3200	Conserved hypothetical protein, putative peptidase, predicted lipoprotein	5	85	47	14	11	4	10	89.6
MHO_3470	P50 = Vaa, surface lipoprotein adhesin	17	17	32	76	18	9	13	51.1
MHO_3490	P60			30					64.2
MHO_3620[b]	P37-like					4			41.8
MHO_3660	P120	25	6	2					119.7
MHO_3720	P75 protein precursor	4	25	65	4	2	4	5	72.4
MHO_3730	Lmp-related protein		27	2					77.8
MHO_4400	Hypothetical protein, predicted lipoprotein						3		29.7
MHO_4720	Hypothetical protein, predicted lipoprotein		2				9	7	28.3

[a]Underlined numbers correspond to the numbers of distinct peptides detected for a nonfragmented lipoprotein. The calculated molecular mass (MM) ignores the signal peptide. E2 and E6 eluates, which did not induce IL-23 production, were analyzed for reference.

[b]MHO_1640 and MHO_3620 were not considered bioactive because they were present solely in the E2 and E6 eluates, which did not induce IL-23 release from hDCs.

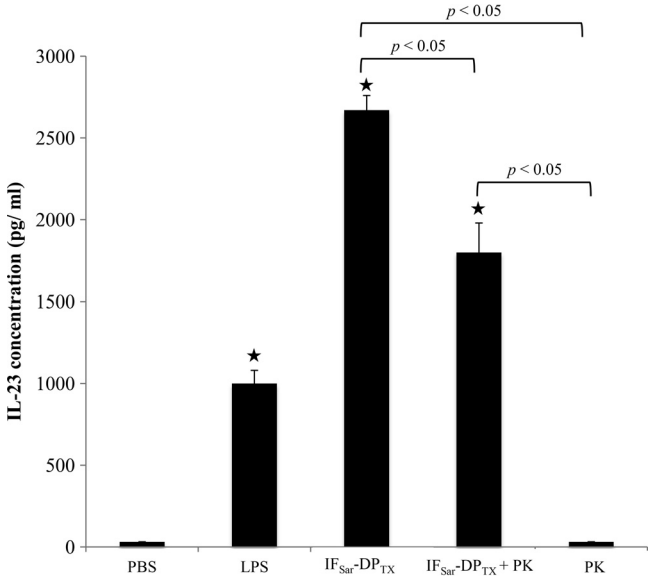

FIG 3 Effect of proteinase K on activity of *M. hominis* PG21 IF_{Sar}-DP_{TX} sequential TX-114 extract. Three independent experiments were performed. ★, significantly different ($P < 0.05$) from PBS according to the Newman-Keuls test. PBS, negative control; LPS, positive control; IF_{Sar}-DP_{TX}, Sarkosyl-insoluble fraction extracted by TX-114 (detergent phase); PK, proteinase K.

IF_{Sar}-DP_{TX} extract was significantly decreased but not abolished. There was no difference between results after 1 h, 4 h, 8 h, and 24 h of proteinase K digestion (data not shown), suggesting that the digestion was complete after 1 h. These data indicate that the protein portion of the lipoproteins only partly contributes to the stimulation of the hDCs and that some proteinase K-resistant compounds, possibly the acylated part of lipoproteins, are major determinants for full expression of this bioactivity.

Stimulation of hDCs by a dendritic cell-stimulating lipopeptide DSL-1 derived from MHO_4720. Because MHO_4720, in contrast to MHO_1730 and MHO_2440, was present in both bioactive eluates E7 and E8, it appeared as an *M. hominis* surface-exposed lipoprotein that could induce IL-23 secretion by hDCs. We aimed at confirming its dendritic cell-activating potency and therefore designed a lipopeptide with a minimal peptidic sequence derived from MHO_4720 that could stimulate IL-23 production by hDCs. We defined the peptide length of the lipopeptide, the amino acid composition, and the acyl chain composition based on data acquired from the analysis of Braun's lipoprotein, the first bacterial lipoprotein characterized in *Escherichia coli* (21). Data and sequence alignments from other bacterial lipoproteins and from bioactive lipopeptides derived from mycoplasmas such as MALP-2 from *M. fermentans*, FSL-1 from *M. salivarium*, and MPPL-1 from *M. pneumoniae*, all known to stimulate immune human cells, were also used (Table 2) (11–13). We eventually synthesized the dendritic stimulating lipopeptide 1 (DSL-1), derived from MHO_4720, which was S-(2,3-bispalmitoyloxypropyl)-cysteine-GGEKFN.

A 10-fold serial dilution of DSL-1 (1 to 1,000 nM) was tested for IL-23 release after coincubation with hDCs. DSL-1 stimulated the production of IL-23 by hDCs at a concentration higher than 10 nM (Fig. 4). The IL-23 production increased up to a DSL-1 concentration of 100 nM and slightly decreased over this concentration. FSL-1 did not induce a significant production of IL-23.

***M. hominis* PG21 induces caspase-dependent IL-1β secretion.** We previously partially described the hDC immune response upon exposure to *M. hominis* PG21 (8). To obtain a deeper understanding of the inflammation response of hDCs, we performed a PCR array targeting the inflammation-related genes of hDCs after 24 h of coincubation with *M. hominis*. A significantly strong upregulation of the IL-1β gene was

TABLE 2 Alignment of N-terminal parts of the 24 potential bioactive lipoproteins of *M. hominis* PG21 and of mycoplasmal bioactive lipopeptides[a]

Gene locus	Species	N-terminal amino acid sequence of protein	MM (kDa)	pI	GRAVY score	Acylation	Reference
MHO_0280	*M. hominis*	C N K T T N H E T N	1,161.2	6.74	−2.070		This study
MHO_0290	*M. hominis*	C K D **P** N K **P** E **V** K	1,157.3	8.18	−1.870		This study
MHO_530	*M. hominis*	C **G G L A I A T T A**	877.0	5.52	1.400		This study
MHO_0540	*M. hominis*	C R F C K K **P** N K Q	1,251.5	9.85	−1.700		This study
MHO_0720	*M. hominis*	C **G** H T **G** T **G** Y **G** F	999.0	6.73	−0.220		This study
MHO_0730	*M. hominis*	C K T **V** N K E K **I** N	1,176.4	9.20	−1.170		This study
MHO_0780	*M. hominis*	C S T T E N S K Y **G**	1,089.1	5.99	−1.310		This study
MHO_0790	*M. hominis*	C S T **T** E N S K Y **G**	1,089.1	5.99	−1.310		This study
MHO_1510	*M. hominis*	C K **I** D P **A** Y E K **G**	1,123.3	6.06	−0.930		This study
MHO_1730	*M. hominis*	C N D **P** K N K K N **P**	1,157.3	9.20	−2.640		This study
MHO_2080	*M. hominis*	C **A I L P** V S C S **L**	1,005.2	5.51	1.990		This study
MHO_2340	*M. hominis*	C **I** K T K K **P** E **V** K	1,173.4	9.63	−1.020		This study
MHO_2440	*M. hominis*	C K T T N D S Q N S	1,097.1	5.83	−1.840		This study
MHO_2620	*M. hominis*	C V K T K K **P** E **G** E	1,118.3	8.18	−1.470		This study
MHO_3070	*M. hominis*	C N N K N S K **L** T K	119.3	9.79	−1.740		This study
MHO_3100	*M. hominis*	C S N K Q D K K E D	1,194.2	6.11	−2.750		This study
MHO_3200	*M. hominis*	C K N T N K K T N N	1,164.3	9.79	−2.460		This study
MHO_3470	*M. hominis*	C N D D K L A E K N	1,149.2	4.56	−1.720		This study
MHO_3490	*M. hominis*	C K K E K E D S Q Q	1,222.3	6.17	−2.750		This study
MHO_3660	*M. hominis*	C T H T N N D E **L** N	1,160.1	4.35	−1.580		This study
MHO_3720	*M. hominis*	C K N E K S N **A** E Y	1,185.2	6.13	−1.960		This study
MHO_3730	*M. hominis*	C T **V** T **V** K V K E K	1,134.4	9.20	−0.150		This study
MHO_4400	*M. hominis*	C N K T **A** T I T **L** N	1,078.2	8.22	−0.040		This study
MHO_4720	*M. hominis*	C **G G** E K **F** N **A F A**	1,043.1	5.99	0.000		This study
MALP-2	*M. fermentans*	C **G** N N D E S N **I** S **F** K E K	2,134.1	4.68	−1.500	Pam2	36
FSL-1	*M. salivarium*	C **G** D **P** K H **P** K S **F**	1,666.1	8.21	−1.360	Pam2	12
MPPL-1	*M. pneumoniae*	C T **G I** Q **A** D **L** R N **L I** K	1,341.5	8.41	−0.133	Pam2	13
P2C-RGDS	*Mycobacterium tuberculosis*	C R G **D** S	1,087.5	5.83	−1.34	Pam2	25
PGTP2-RL	*Porphyromonas gingivalis*	C N S Q **A** K	649.7	8.22	−1.233	Pam3	37
Murein LPP	*E. coli*	C S S N K **I** D E **L** S D D	1,325.3	3.84	−1.083	Pam3	21
MDPL	*M. synoviae*	C **G** D Q T **P A P** E P T **P G** N	1,383	3.67	−1.307	Pam2	38
DSL-1	*M. hominis*	C **G G** E K **F** N	753.8	5.99	−0.914	Pam2	This study

[a]Molecular mass (MM), isoelectric point (pI), and GRAVY score were determined using ProtParam software (http://web.expasy.org/cgi-bin/protparam/protparam). Hydrophobic amino acids are in boldface. Pam, palmitic acid; Pam2, diacylated lipoproteins with two palmitic acids; Pam3, triacylated lipoproteins with three palmitic acids.

observed, suggesting the activation of the inflammasome (data not shown). We confirmed the strong IL-1β release after 24 h of coincubation of *M. hominis* with hDCs by ELISA (Fig. 5A). A weaker IL-1β release was observed after 4 h of coincubation. IL-1β release was also observed after exposure of hDCs to *M. hominis* fractions enriched in

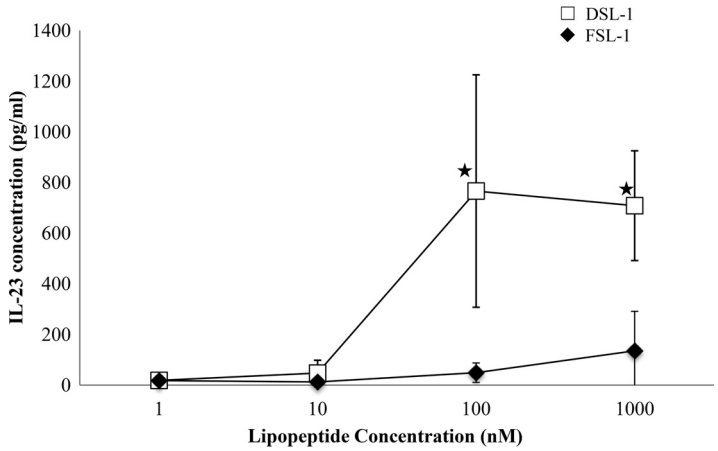

FIG 4 Release of IL-23 by hDCs after coincubation with DSL-1 and FSL-1. Results are shown as the means and standard errors of the means from four independent experiments. ★, significantly different ($P < 0.05$) from IL-23 concentration after coincubation with 1 nM or 10 nM DSL-1 according to the Newman-Keuls test.

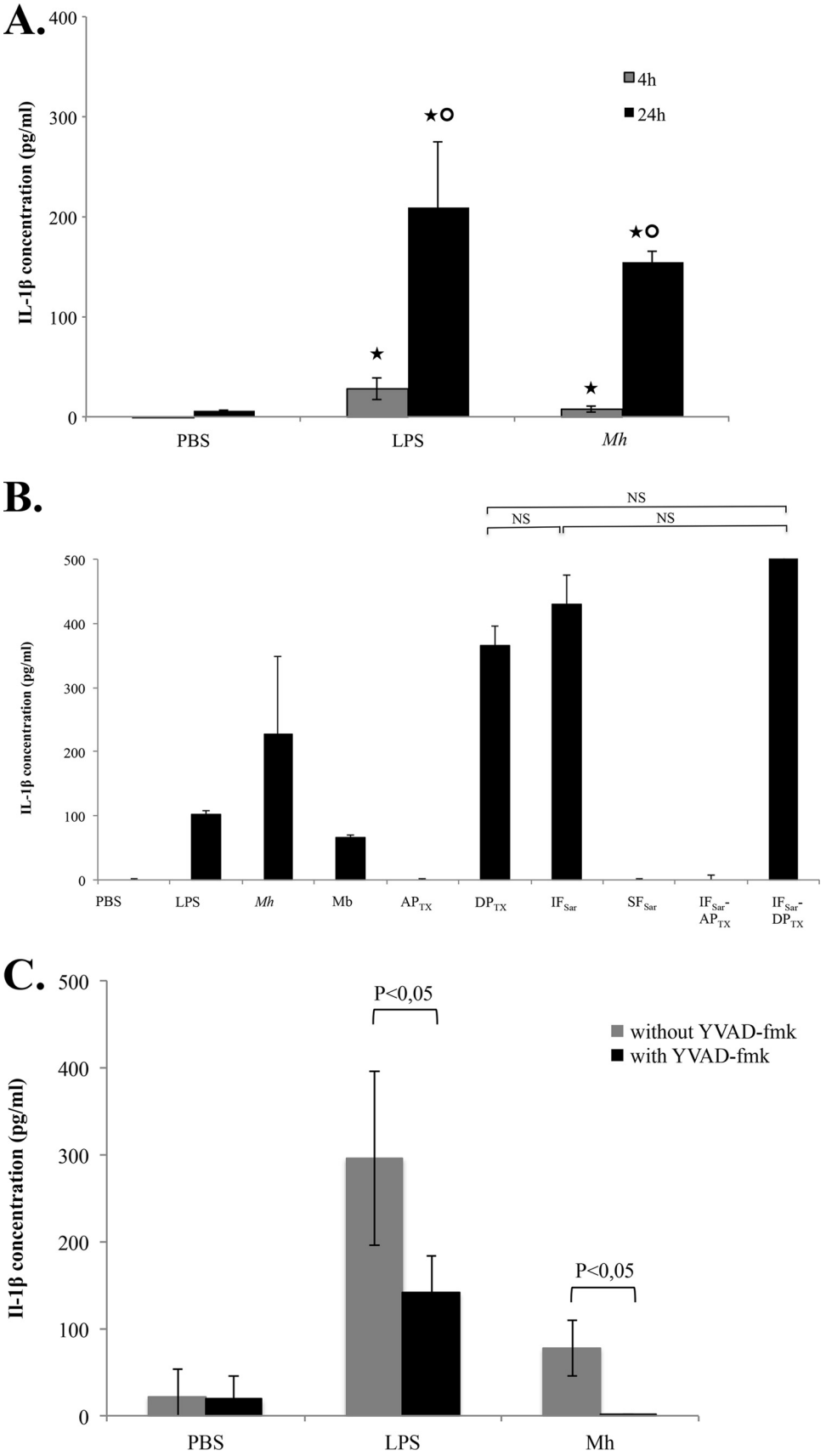

FIG 5 IL-1β release by hDCs. (A) Results after incubation with *M. hominis* PG21 for 4 h and 24 h. ★, significantly different ($P < 0.05$) from IL-1β concentration released after coincubation with PBS at the same time point; ○,

(Continued on next page)

lipoproteins, especially the sequential extract IF_{Sar}-DP_{TX} (Fig. 5B). To determine whether caspases were involved in this IL-1β release, a caspase-1- and caspase-5-specific inhibitor, Ac-YVAD-fmk, was added to the hDCs before a 24-h coincubation with *M. hominis* (Fig. 5C). IL-1β release was abolished when the cells were exposed beforehand to Ac-YVAD-fmk, suggesting that caspase-1 and/or caspase-5 was involved in IL-1β production by hDCs after coincubation with *M. hominis*.

To assess which caspase and what other inflammasome components were activated in hDCs, we performed a PCR array targeting inflammasome genes after 4 h and 24 h of coincubation with *M. hominis*. The expression of 85 hDC genes involved in inflammasome activation was quantified in hDCs alone and in hDCs coincubated with *M. hominis* PG21 (Table 3). As expected, a strong upregulation of the IL-1β gene and of the IL-12β genes (IL-23 subunit gene) was observed (fold changes, 285 and 2,660, respectively, at 24 h). There was no change in the IL-18-encoding gene expression. The IL-6 inflammatory cytokine and NF-κB genes were also upregulated at 24 h. Among the caspase-coding genes tested, only the caspase-5 gene was upregulated at 4 h and 24 h, whereas there was no variation of the caspase-1 and caspase-8 gene expression. In the NOD-like receptor (NLR) family, the expression levels of NLRX1-, NOD1-, and NOD2-coding genes were downregulated at 4 h, and the expression level of NLRP3 was downregulated at 24 h (fold change, −21.8). The gene encoding the adaptor protein PYCARD was also downregulated at 24 h (fold change, −23.7). The expression level of the NLRP7-coding gene was assessed by reverse transcription-quantitative PCR (qRT-PCR) but did not show any change upon exposure of hDCs to *M. hominis*. No upregulation of NLR was observed at 4 h or at 24 h of coincubation. Taken together, these data suggest that *M. hominis* PG21 may activate the inflammasome and induce IL-1β release in a caspase-5-dependent manner.

In addition, the prostaglandin-endoperoxide synthase 2 (COX2)-encoding gene, *ptgs2*, was upregulated at 4 h (fold change, 4.7) and highly upregulated at 24 h (fold change, 152.6). Chemoattractant-coding genes were also regulated, with an increased expression of the CCL5-encoding gene at 4 h and an increased expression of CCL2- and CXCL1-encoding genes at 24 h.

DISCUSSION

Identification of IL-23 release-inducing lipoproteins in a sequential Sarkosyl/TX-114 extract of *M. hominis* PG21. In the present study, 24 lipoproteins from the bioactive eluates of the IF_{Sar}-DP_{TX} sequential extract were identified and divided into two groups: lipoproteins with apparent molecular masses ranging from 20 to 35 kDa and from 40 to 100 kDa. These data suggest that IL-23 production by hDCs results either from the action of several lipoproteins or from the action of different forms of the same lipoprotein (whole or fragmented). As a comparison, three fractions (from 22 to 25 kDa, from 25 to 32 kDa, and from 36 to 43 kDa) from *Mycoplasma arthritidis*, a mycoplasma phylogenetically close to *M. hominis*, were able to induce TNF-α secretion by murine monocytes (2). Peltier et al. showed that the stimulation of TNF-α production by THP-1 cells after incubation with *M. hominis* PG21 fractions was due to proteins that had molecular masses from 10 to 50 kDa (3). Hasebe et al. isolated and purified a lipoprotein of 40 kDa from *M. hominis* membranes that stimulated TNF-α production by THP-1 cells (14). This study reports for the first time that a group of high-molecular-mass lipoproteins from *M. hominis* could be involved in the immune response of hDCs.

FIG 5 Legend (Continued)
significantly different ($P < 0.05$) from IL-1β concentration released after coincubation for 4 h according to the Newman-Keuls test. (B) Results after incubation with *M. hominis* PG21 and its detergent fractions. (C) Results after coincubation with *M. hominis* PG21 with and without the caspase inhibitor YVAD-fmk. *Mh*, *M. hominis* PG21. Results are shown as the means and standard errors of the means from three independent experiments. PBS, negative control; LPS, positive control; *Mh*, *M. hominis* PG21; Mb, *M. hominis* PG21 membranes; AP_{TX}, TX-114 aqueous phase (nonextracted proteins); DP_{TX}, TX-114 detergent phase (extracted proteins); IF_{Sar}, Sarkosyl-insoluble fraction (nonextracted proteins); SF_{Sar}, Sarkosyl-soluble fraction (extracted proteins); IF_{Sar}-DP_{TX}, Sarkosyl-insoluble fraction extracted by TX-114 (detergent phase); IF_{Sar}-AP_{TX}, Sarkosyl-insoluble fraction extracted by TX-114 (aqueous phase); NS, statistically nonsignificant according to the Newman-Keuls test.

TABLE 3 Differential expression of the hDC inflammasome genes after 4 h and 24 h of coincubation with *M. hominis* PG21[a]

Protein name	*t* = 4 h		*t* = 24 h	
	Fold change	*P* value	Fold change	*P* value
Absent in melanoma 2	0.7	0.269	4.3	0.057
B-cell CLL/lymphoma 2	**4.4**	**0.036**	**20.7**	**0.034**
BCL2-like 1	1.4	0.100	3.4	0.059
Baculoviral IAP repeat containing 2	1.2	0.577	**3.5**	**0.039**
Baculoviral IAP repeat containing 3	2.1	0.708	**34.7**	**0.029**
Caspase recruitment domain family, member 18	Undetected	Undetected	Undetected	Undetected
Caspase recruitment domain family, member 6	−1.7	0.309	−1.7	0.155
Caspase 1, apoptosis-related cysteine peptidase (interleukin 1β convertase)	1.1	0.677	1.1	0.767
Caspase 5, apoptosis-related cysteine peptidase	**3.1**	**0.019**	**5.8**	**0.030**
Caspase 8, apoptosis-related cysteine peptidase	−1.8	0.492	−1.2	0.412
Chemokine (C-C motif) ligand 2	1.1	0.975	**80.9**	**0.010**
Chemokine (C-C motif) ligand 5	**30.3**	**0.042**	35.1	0.221
Chemokine (C-C motif) ligand 7	−1.1	0.720	Undetected	Undetected
CD40 ligand	−4.3	0.401	−2.1	0.205
CASP8 and FADD-like apoptosis regulator	1.7	0.604	**5.9**	**0.024**
Conserved helix-loop-helix ubiquitous kinase	−1.1	0.332	1.6	0.467
Class II major histocompatibility complex, transactivator	−1.1	0.938	**−4.3**	**0.024**
Cathepsin B	1.0	0.999	**−2.8**	**0.011**
Chemokine (C-X-C motif) ligand 1 (melanoma growth stimulating activity alpha)	**2.0**	**0.038**	**934.5**	**0.031**
Chemokine (C-X-C motif) ligand 2	1.0	0.540	265.2	0.054
Fas (TNFRSF6)-associated via death domain	−2.0	0.254	1.0	0.978
Heat shock protein 90kDa alpha (cytosolic), class A member 1	−1.2	0.317	−1.3	0.296
Heat shock protein 90kDa alpha (cytosolic), class B member 1	1.0	0.905	−1.9	0.150
Heat shock protein 90kDa beta (Grp94), member 1	−1.2	0.250	−1.1	0.848
Interferon beta 1 fibroblast	−2.4	0.570	Undetected	Undetected
Interferon gamma	Undetected	Undetected	Undetected	Undetected
Inhibitor of kappa light polypeptide gene enhancer in B cells. kinase beta	1.1	0.711	1.2	0.585
Inhibitor of kappa light polypeptide gene enhancer in B cells. kinase gamma	−1.2	0.659	1.2	0.500
Interleukin 12A (natural killer cell stimulatory factor 1, cytotoxic lymphocyte maturation factor 1, p35)	Undetected	Undetected	Undetected	Undetected
Interleukin 12B (natural killer cell stimulatory factor 2, cytotoxic lymphocyte maturation factor 2, p40)	**43.4**	**0.010**	**2,660.2**	**0.018**
Interleukin 18 (interferon-gamma-inducing factor)	−1.5	0.319	1.7	0.435
Interleukin 1β	**8.0**	**0.040**	**285.5**	**0.035**
Interleukin 33	Undetected	Undetected	Undetected	Undetected
Interleukin 6 (interferon beta 2)	−1.1	0.973	**4,784.0**	**0.016**
Interleukin-1 receptor-associated kinase 1	1.4	0.482	−1.3	0.385
Interferon regulatory factor 1	1.8	0.184	**8.8**	**0.040**
Interferon regulatory factor 2	1.2	0.811	**2.7**	**0.046**
Mitogen-activated protein kinase kinase kinase 7	−1.3	0.185	−1.1	0.455
Mitogen-activated protein kinase 1	−1.2	0.729	−1.2	0.299
Mitogen-activated protein kinase 11	1.4	0.138	**3.5**	**0.047**
Mitogen-activated protein kinase 12	2.0	0.105	−1.9	0.202
Mitogen-activated protein kinase 13	1.0	0.999	**2.6**	**0.047**
Mitogen-activated protein kinase 3	−1.5	0.623	**−3.8**	**0.035**
Mitogen-activated protein kinase 8	1.0	0.792	**3.3**	**0.021**
Mitogen-activated protein kinase 9	−1.2	0.523	**−2.9**	**0.038**
Mediterranean fever	1.9	0.055	−2.2	0.111
Myeloid differentiation primary response gene (gene 88 product)	−1.4	0.630	1.3	0.112
NLR family, apoptosis inhibitory protein	−2.7	0.478	**−12.2**	**0.026**
Nuclear factor of kappa light polypeptide gene enhancer in B cells 1	2.3	0.537	**11.5**	**0.010**
Nuclear factor of kappa light polypeptide gene enhancer in B cells inhibitor. alpha	2.2	0.473	**6.5**	**0.018**
Nuclear factor of kappa light polypeptide gene enhancer in B cells inhibitor. beta	1.8	0.139	1.7	0.073
NLR family, CARD domain containing 4	−1.1	0.782	−2.3	0.069
NLR family, CARD domain containing 5	1.0	0.822	1.9	0.166
NLR family, pyrin domain containing 1	1.5	0.352	1.3	0.590
NLR family, pyrin domain containing 12	1.9	0.284	Undetected	Undetected
NLR family, pyrin domain containing 3	−1.1	0.952	**−21.8**	**0.030**
NLR family, pyrin domain containing 4	Undetected	Undetected	Undetected	Undetected
NLR family, pyrin domain containing 5	Undetected	Undetected	Undetected	Undetected

(Continued on next page)

TABLE 3 (Continued)

Protein name	$t = 4$ h		$t = 24$ h	
	Fold change	*P* value	Fold change	*P* value
NLR family, pyrin domain containing 6	Undetected	Undetected	Undetected	Undetected
NLR family, pyrin domain containing 7[b]	0.9	0.788	1.9	0.329
NLR family, pyrin domain containing 9	−1.3	0.719	1.3	0.414
NLR family member X1	**−5.4**	**0.034**	−2.1	0.280
Nucleotide-binding oligomerization domain containing 1	**−8.2**	**0.004**	−1.3	0.276
Nucleotide-binding oligomerization domain containing 2	**−6.0**	**0.030**	−1.2	0.668
Purinergic receptor P2X, ligand-gated ion channel, 7	18.6	0.070	7.2	0.064
Pannexin 1	−1.3	0.267	**2.9**	**0.017**
Phosphoprotein enriched in astrocytes 15	1.1	0.665	2.0	0.233
Proline-serine-threonine phosphatase interacting protein 1	−1.9	0.352	**−13**	**0.029**
Prostaglandin-endoperoxide synthase 2 (prostaglandin G/H synthase and cyclooxygenase)	**4.7**	**0.033**	**152.6**	**0.032**
PYD and CARD domain containing	−2.3	0.204	**−23.7**	**0.045**
PYD (pyrin domain) containing 1	1.5	0.507	3.2	0.920
Renal tumor antigen	**−1.3**	**0.038**	−1.3	0.314
V-rel reticuloendotheliosis viral oncogene homolog A (avian)	**0.5**	**0.031**	**2.2**	**0.045**
Receptor-interacting serine-threonine kinase 2	2.1	0.579	**9.5**	**0.023**
SGT1, suppressor of G2 allele of SKP1 (*Saccharomyces cerevisiae*)	−1.1	0.652	1.1	0.157
TGF-beta activated kinase 1/MAP3K7 binding protein 1	−2.6	0.490	**−1.6**	**0.038**
TGF-beta activated kinase 1/MAP3K7 binding protein 2	−1.2	0.756	**2.6**	**0.027**
Toll-interleukin 1 receptor (TIR) domain containing adaptor protein	−1.6	0.437	−1.9	0.264
Tumor necrosis factor	2.4	0.489	7.6	0.110
Tumor necrosis factor (ligand) superfamily, member 11	Undetected	Undetected	Undetected	Undetected
Tumor necrosis factor (ligand) superfamily, member 14	4.0	0.054	1.4	0.350
Tumor necrosis factor (ligand) superfamily, member 4	1.0	0.861	**38.7**	**0.006**
TNF receptor-associated factor 6	−1.2	0.140	1.6	0.121
Thioredoxin interacting protein	−1.5	0.062	−3.3	0.264
X-linked inhibitor of apoptosis	1.0	0.979	**2.4**	**0.041**

[a]The lipoproteins for which significant fold changes (P value < 0.05) were observed are in boldface. Three independent biological replicates were performed for each time point.

[b]The expression level of the NLRP7-coding gene, not present in the PCR Human Inflammasome (Qiagen) array, was determined by qRT-PCR.

Among the 24 potential bioactive lipoproteins, we focused on MHO_4270 because this lipoprotein could alone be responsible for the bioactivity of the E7 and E8 eluates. Many orthologs of this hypothetical lipoprotein were found in other mycoplasmal species, such as *Mycoplasma spumans*, *M. canadense*, *M. alkalescens*, and *M. arginini*, involved in animal infections. These hypothetical proteins and lipoproteins are all of unknown function. However, a leucine-rich repeat (LRR) domain is conserved among all these lipoproteins. The LRR domain is a widespread sequence of 20 to 30 amino acids with a characteristic repetitive sequence pattern rich in leucines. The LRR corresponds to a short β-strand and α-helix region, which is involved in protein-protein interactions (22). Indeed, it was reported that mycoplasma diacylated lipoproteins and FSL-1, an *M. salivarium*-derived diacylated lipopeptide, were recognized via their LRR domain by the LRR domain of the Toll-like receptor 2 (TLR2) (23). As TLR2 was previously reported to interact with *M. hominis* (8), we can speculate that MHO_4720 could interact via its LRR domain with TLR2 of the hDCs.

Lipopeptide DSL-1, corresponding to the N-terminal part of MHO_4720, stimulates IL-23 release by hDCs. We noted that the protein moiety was important to stimulate hDCs because proteinase K digestion significantly reduced the bioactivity of the sequential extract IF_{Sar}-DP_{TX}. Peltier et al. also showed that the activity of the stimulating factor of THP-1 cells present in a TX-114 extract from *M. hominis* was significantly decreased by proteinase K digestion (3). To determine if a minimal lipoprotein structure could stimulate the hDCs, we designed a synthetic lipopeptide. As suggested for the generation of the bioactive lipopeptide MPPL-1 from *M. pneumoniae* (13), we first attempted to find a consensus sequence by the alignment of the N-terminal sequence of the 24 potential bioactive lipoproteins identified in the present study. However, no consensus sequence could be identified. Synthetic lipopeptides derived from Braun's lipoprotein were shown to exhibit stimulatory activity comparable

to that of native lipoproteins (24). It was also shown that a TLR2 agonist, which is the hDC TLR that recognizes *M. hominis* (8), required a hydrophilic N-terminal part (25). The DSL-1 peptide chosen had seven N-terminal amino acid residues (CGGEKFN), which conferred a negative grand average of hydropathy (GRAVY) score close to that of the bioactive mycoplasmal lipopeptides FSL-1 and MALP-2 (11, 12) (Table 2). In addition, the presence of only two acyl chains bound to the cysteine residue would be adequate for the bioactivity because many mycoplasmal bioactive lipopeptides such as FSL-1, MALP-2, and MPPL-1 are diacylated (11–13).

DSL-1 induced IL-23 production in two stages, an increasing stage followed by a steady-state stage. Okusawa et al. also observed two phases in the production of IL-6, IL-8, and MCP-1 by human gingival fibroblasts stimulated by FSL-1 and in the production of TNF-α by THP-1 cells induced by FSL-1 and MALP-2 (26). In addition, FSL-1 failed to induce significant IL-23 production, highlighting that the immune hDC response was specific to the DSL-1 lipopeptide.

***M. hominis* PG21 activates the hDC inflammasome.** Results of the PCR array targeting inflammasome genes were validated by the strong upregulation of the IL-23- and IL-1β-coding genes, which confirmed the IL-23 and IL-1β release observed in coincubation supernatants. The increase of the transcription of the IL-6 gene was also confirmed by IL-6 ELISA detection in the supernatants after coincubation (data not shown). IL-1β release after coincubation of *M. hominis* with hDCs may result from caspase-5-dependent inflammasome activation. However, the role of caspase-1 in the IL-1β release observed after coincubation of hDCs with *M. hominis* cannot be ruled out. Caspase-1 could be constitutively expressed, as it was shown to be the case in the monocytic cell line THP-1 (27). In addition, caspase-1 and caspase-5 were both reported to be recruited by the NLRP1/PYCARD complex and were reported to be capable of forming heterocomplexes in the THP1 cell line stimulated by LPS or phorbol myristate acetate (PMA) (28).

In the present study, the inflammasome sensor remained unidentified at the gene expression level among the 13 NLR genes tested. The NLR protein family comprises 22 members in humans; therefore, we can speculate that either the sensor is part of the 9 untested NLRs or the molecule does not trigger a priming step of gene expression; rather, it may directly activate NLR(s) at the protein level to assemble the inflammasome. The NLRP7-encoding gene was not regulated in our model of coincubation, although (i) NLRP7 had been specifically identified as an intracellular sensor of mycoplasmal acylated lipoproteins and (ii) NLRP7 was reported to activate the inflammasome of the THP-1 cell line after exposure to *A. laidlawii*, to lipopeptides derived from mycoplasmas such as FSL-1 and MALP-2, and to the synthetic lipopeptides Pam_2CSK4 and Pam_3CSK4 (16). Notably, we observed a significant downregulation of the NLRP3-encoding gene and of the adaptor PYCARD-coding gene at 24 h. The ability of LPS to activate NLRP3 was described to be weak and transient, with a low capacity of NLRP3 activation after 24 h (29). Chronic LPS stimulation was also reported to trigger IL-10-dependent regulatory mechanisms. Similarly, we previously showed that *M. hominis* PG21 induces IL-10 release after coincubation with the hDCs (8). In the present study, an early time point (4 h) and a late time point (24 h) were chosen to assess major differences in the transcriptional levels of individual genes. At 4 h, we might have missed the upregulation of the NLRP3 gene. In addition, even though we did not observe a modulation of NLRP3 gene expression at 4 h, a small amount of constitutively expressed NLRP3 protein might be sufficient to activate and trigger inflammasome assembly. In addition, for several other mycoplasma species, the NLRP3 protein is the sensor of the inflammasome. Indeed, *M. pneumoniae* community-acquired respiratory distress syndrome (CARDS) toxin, *A. laidlawii*, *M. hyorhinis*, and *M. salivarium* were reported to activate the NLRP3 inflammasome of mouse primary bone marrow-derived macrophages (30), of human THP-1 cells (16, 17), and of murine dendritic cells (18), respectively. For all these reasons, NLRP3 may be the inflammasome receptor involved in the caspase-dependent IL-1β release.

We observed an upregulation of the prostaglandin-endoperoxide synthase 2 (COX-2)-encoding gene at 24 h. The COX-2-inducible enzyme is responsible for the synthesis of prostaglandin E2 (PGE2) from arachidonic acid derived from membrane phospholipids. PGE2 is a potent lipid mediator involved in maintaining homeostasis but also in promoting acute inflammation or immune suppression in chronic inflammation. The overexpression of COX-2 in human placental trophoblast cells was previously described to be induced by MALP-2, a mycoplasmal lipopeptide (31). Moreover, in the present study, the overexpression of COX-2 may be related to the downregulation of NLRP3. In accordance with this hypothesis, an inverse relation between the expression of COX-2 and NLRP3 was previously reported in human primary monocyte-derived macrophages (32).

Conclusion. We studied the interaction of *M. hominis* PG21 with hDCs by analyzing both sides of the interaction, the mycoplasmal lipoproteins that induce IL-23 production and the cell innate immune response. We defined a list of 24 lipoproteins that could induce the secretion of IL-23 by hDCs. Among them, lipoprotein MHO_4720 was identified as a potential stimulating factor of hDCs. Inflammasome activation of hDCs with caspase-5-dependent production of IL-1β was also observed. After 24 h of coincubation, a downregulation of NLRP3- and of the adaptor PYCARD-encoding genes associated with an upregulation of the COX2-encoding gene suggests a regulation of the inflammasome and a potential involvement of NLRP3 as an inflammasome sensor. Further studies are necessary to specify the role of NLRP3 in hDC inflammasome activation after incubation with *M. hominis* PG21.

MATERIALS AND METHODS

Growth of bacteria and membrane preparations. *M. hominis* strain PG21 (ATCC 23114) was cultivated, and membranes were isolated as described previously (8) with slight modifications. Briefly *M. hominis* was harvested by centrifugation (20,000 $\times$ *g*, 30 min, 4°C) and washed three times in phosphate-buffered saline (PBS). The cells were lysed by three 1-min bursts of sonication on ice at the maximum setting for the micro tip (Vibra-Cell sonicator; Branson). Membranes were recovered by centrifugation for 1 h at 30,000 $\times$ *g* (4°C). The pellets were dispersed in PBS and washed in the same buffer four times. The final pellets were resuspended in PBS.

Membrane protein extraction. *M. hominis* PG21 membranes were separated into detergent-soluble and detergent-insoluble fractions using five detergents: 3-[(3-cholamidopropyl) dimethylammonio]-1-propanesulfonate (CHAPS), 50 nM (Thermo Fisher Scientific, San Jose, CA); octyl-glucopyranoside (OG), 75 nM (Sigma-Aldrich, St. Louis, MO); sodium deoxycholate (DOC), 50 nM (Sigma-Aldrich); Triton X-100 (TX-100), 1% (Sigma-Aldrich); *N*-lauroylsarcosine sodium salt (Sarkosyl), 100 nM (Sigma-Aldrich); and 1% TX-114 (Sigma-Aldrich). One volume of membrane suspension (1 mg of protein/ml) was mixed with 4 volumes of detergent in 0.1 M sodium phosphate buffer (pH 7.4) and gently rocked for 1 h at 4°C. The mixtures were centrifuged at 285,000 $\times$ *g* for 15 min at 4°C (Beckman TL-100 ultracentrifuge, TLA 100.1 rotor) to separate the solubilized proteins from the insoluble material. For the sequential extraction procedure using two detergents, the Sarkosyl-soluble fraction (SF_{Sar}) and the Sarkosyl-insoluble fraction (IF_{Sar}) were subjected to TX-114 1% extraction. A volume of 900 μl of ice-cold acetone was added to 100 μl of sample (final detergent extract) to precipitate the proteins. The proteins were further washed using ice-cold acetone. The protein concentration was determined using the DC protein assay kit (Bio-Rad, Hercules, CA).

Preparative SDS-PAGE experiments. Each detergent-soluble and detergent-insoluble fraction obtained from a quantity of 200 μg of total membrane protein was heated for 3 min at 100°C and then separated on a 12.5% acrylamide gel by SDS-PAGE. The proteins were visualized using the ProteoSilver silver stain kit (Sigma-Aldrich).

To identify the lipoproteins present in the IF_{Sar}-DP_{TX} sequential extract (i.e., the TX-114 detergent-enriched phase obtained by extraction of the Sarkosyl-insoluble fraction), the extract was separated by 12.5% SDS-PAGE. The gel was cut into 10 equal bands, and each band was eluted with 75 nM OG. The proteins were precipitated using ice-cold acetone (9 volumes of acetone for 1 volume of sample). This precipitation step allowed the removal of OG. The protein pellet was further washed using ice-cold acetone before being dissolved in PBS. Each eluate was incubated with hDCs for 24 h as described below.

Proteins from the eluates of interest were identified as previously described by liquid chromatography-tandem mass spectrometry (LC-MS/MS) (19).

Proteinase K digestion of the IF_{Sar}-DP_{TX} sequential extract. The IF_{Sar}-DP_{TX} sequential extract was incubated with 0.4 U proteinase K coupled to EupergitC (Sigma-Aldrich), which is a carrier consisting of macroporous beads for immobilizing enzymes, and gently rocked for 1 h at 37°C. The insoluble enzyme was subsequently removed by centrifugation at 800 $\times$ *g* for 5 min. The digested extracts were tested for IL-23 release after coincubation with hDCs.

Design and activity of DSL-1. *In silico* analysis of the N-terminal part of the hypothetical bioactive lipoproteins from eluates E3, E4, E5, E7, and E8 was performed using Molligen 3.0 software (http://www.cbib.u-bordeaux2.fr/outils/molligen/) (33). The search for a consensus peptide sequence was carried out using ClustalW2 software (http://www.ebi.ac.uk/Tools/msa/clustalw2/). The hydropathy (GRAVY scores)

of the peptidic fragments was determined using ProtParam software (http://web.expasy.org/cgi-bin/protparam/protparam). FSL-1, S-(2,3-bispalmitoyloxypropyl)-CGDPKHSPKSF, synthesized on the basis of a 44-kDa lipoprotein of *M. salivarium* (12), and S-(2,3-bispalmitoyloxypropyl)-CGGEKFN (DSL-1) were synthesized by EMC microcollections GmbH (Tübingen, Germany). The DSL-1 purity was confirmed by analytical high-performance liquid chromatography (HPLC) with a reverse-phase (RP) C_{18} column, and the mass of the synthetic product was checked by electrospray ionization mass spectrometry (ESI-MS) (see Fig. S1 in the supplemental material). A 1-mg/ml stock solution was prepared in PBS.

Human monocyte-derived DC generation and *M. hominis* stimulation. Human monocyte-derived DC generation was performed as described elsewhere (8). Briefly, human monocytes were selected from human peripheral blood mononuclear cells (PBMC) using CD14 microbeads (Miltenyi Biotec, San Diego, CA). Plastic-adherent monocytes were cultured for 5 days with 25 ng/ml of human granulocyte-macrophage colony-stimulating factor (hGM-CSF) and 10 ng/ml of human interleukin-4. The purity and viability of DC preparation were >95%. For IL-23 and IL-1β release analysis, hDCs were transferred into 96-well plates at 5×10^5 cells per well along with the different extracts at 20 μg/ml, except for the sequential extractions, for which the protein concentrations were lower and could not be adjusted. An *M. hominis* suspension at 10^8 color changing units (CCU)/ml for a multiplicity of infection of 50, LPS from *Escherichia coli* serotype O26:B6 (Sigma-Aldrich) at 10 ng/ml, and mycoplasma membranes at 20 μg/ml were used. The mixtures were incubated at 37°C for 24 h. The cells were pelleted by centrifugation at 1,300 $\times$ *g* for 10 min at room temperature. The supernatants were collected for the determination of IL-23 and IL-1β using the human ELISA Ready-Set-Go system (eBioscience, San Diego, CA). The cell viability was assessed using trypan blue (Sigma-Aldrich). When appropriate, the caspase-1 and -5 inhibitor, Ac-YVAD-fmk (40 μM; Miltenyi Biotec), was added to the cells 30 min before coincubation of the hDCs with *M. hominis*. At least three independent biological replicates were performed for each quantitative analysis.

RNA extraction, reverse transcription, and PCR array. To evaluate the differential expression of hDC genes upon contact with *M. hominis*, hDCs were coincubated with *M. hominis* as described above at 37°C for 4 and 24 h. After coincubation, the cells were pelleted, total RNA was extracted from the pellet, and the RNA purity and integrity were assessed as previously described (19).

The differential expression of hDC genes was determined using the Human Inflammatory Response & Autoimmunity and the Human Inflammasomes PCR arrays (Qiagen, Hilden, Germany). The amplification settings, cycle threshold (C_T) determination, and expression ratios were determined as previously described (19). The limit of detection and C_T cutoff were 35 for each gene, as recommended by the manufacturer. The expression level of the NLRP7-encoding gene, not present in the PCR array, was determined by qRT-PCR with previously reported primers (34) and the same PCR conditions as for the PCR arrays.

Statistics. The *P* values were calculated based on analysis of variance (ANOVA) and the Newman-Keuls test as the *post hoc* test in ELISAs. For the expression ratios of hDC genes, the *P* values were calculated based on Student's *t* test of the ΔC_T values between hDCs incubated with *M. hominis* PG21 and hDCs incubated without *M. hominis*, independently for each gene (35). A *P* value of <0.05 was considered significant.

SUPPLEMENTAL MATERIAL

Supplemental material for this article may be found at https://doi.org/10.1128/JB.00213-17.

SUPPLEMENTAL FILE 1, PDF file, 0.5 MB.

ACKNOWLEDGMENT

This study was supported by internal funding.

REFERENCES

1. Browning GF, Marenda MS, Noormohammadi AH, Markham PF. 2011. The central role of lipoproteins in the pathogenesis of mycoplasmoses. Vet Microbiol 153:44–50. https://doi.org/10.1016/j.vetmic.2011.05.031.
2. Cole BC, Mu HH, Pennock ND, Hasebe A, Chan FV, Washburn LR, Peltier MR. 2005. Isolation and partial purification of macrophage- and dendritic cell-activating components from *Mycoplasma arthritidis*: association with organism virulence and involvement with Toll-like receptor 2. Infect Immun 73:6039–6047. https://doi.org/10.1128/IAI.73.9.6039-6047.2005.
3. Peltier MR, Freeman AJ, Mu HH, Cole BC. 2005. Characterization and partial purification of a macrophage-stimulating factor from *Mycoplasma hominis*. Am J Reprod Immunol 54:342–351. https://doi.org/10.1111/j.1600-0897.2005.00316.x.
4. Shimizu T, Kida Y, Kuwano K. 2007. Triacylated lipoproteins derived from *Mycoplasma pneumoniae* activate nuclear factor-kappaB through toll-like receptors 1 and 2. Immunology 121:473–483. https://doi.org/10.1111/j.1365-2567.2007.02594.x.
5. Shimizu T, Kida Y, Kuwano K. 2008. *Ureaplasma parvum* lipoproteins, including MB antigen, activate NF-kappaB through TLR1, TLR2 and TLR6. Microbiology 154:1318–1325. https://doi.org/10.1099/mic.0.2007/016212-0.
6. Shimizu T, Kida Y, Kuwano K. 2008. A triacylated lipoprotein from *Mycoplasma genitalium* activates NF-kappaB through Toll-like receptor 1 (TLR1) and TLR2. Infect Immun 76:3672–3678. https://doi.org/10.1128/IAI.00257-08.
7. He J, You X, Zeng Y, Yu M, Zuo L, Wu Y. 2009. *Mycoplasma genitalium*-derived lipid-associated membrane proteins activate NF-kappaB through toll-like receptors 1, 2, and 6 and CD14 in a MyD88-dependent pathway. Clin Vaccine Immunol 16:1750–1757. https://doi.org/10.1128/CVI.00281-09.
8. Truchetet ME, Béven L, Renaudin H, Douchet I, Férandon C, Charron A, Blanco P, Schaeverbeke T, Contin-Bordes C, Bébéar C. 2011. Potential role of *Mycoplasma hominis* in interleukin (IL)-17-producing CD4+ T-cell generation via induction of IL-23 secretion by human dendritic cells. J Infect Dis 204:1796–1805. https://doi.org/10.1093/infdis/jir630.
9. Calcutt MJ, Kim MF, Karpas AB, Muhlradt PF, Wise KS. 1999. Differential posttranslational processing confers intraspecies variation of a major

surface lipoprotein and a macrophage-activating lipopeptide of *Mycoplasma fermentans*. Infect Immun 67:760–771.
10. Liu YC, Lin IH, Chung WJ, Hu WS, Ng WV, Lu CY, Huang TY, Shu HW, Hsiao KJ, Tsai SF, Chang CH, Lin CH. 2012. Proteomics characterization of cytoplasmic and lipid-associated membrane proteins of human pathogen *Mycoplasma fermentans* M64. PLoS One 7:e35304. https://doi.org/10.1371/journal.pone.0035304.
11. Muhlradt PF, Kiess M, Meyer H, Sussmuth R, Jung G. 1997. Isolation, structure elucidation, and synthesis of a macrophage stimulatory lipopeptide from *Mycoplasma fermentans* acting at picomolar concentration. J Exp Med 185:1951–1958. https://doi.org/10.1084/jem.185.11.1951.
12. Shibata K, Hasebe A, Into T, Yamada M, Watanabe T. 2000. The N-terminal lipopeptide of a 44-kDa membrane-bound lipoprotein of *Mycoplasma salivarium* is responsible for the expression of intercellular adhesion molecule-1 on the cell surface of normal human gingival fibroblasts. J Immunol 165:6538–6544. https://doi.org/10.4049/jimmunol.165.11.6538.
13. Into T, Dohkan J, Inomata M, Nakashima M, Shibata K, Matsushita K. 2007. Synthesis and characterization of a dipalmitoylated lipopeptide derived from paralogous lipoproteins of *Mycoplasma pneumoniae*. Infect Immun 75:2253–2259. https://doi.org/10.1128/IAI.00141-07.
14. Hasebe A, Mu HH, Cole BC. 2014. A potential pathogenic factor from *Mycoplasma hominis* is a TLR2-dependent, macrophage-activating, P50-related adhesin. Am J Reprod Immunol 72:285–295. https://doi.org/10.1111/aji.12279.
15. Shimizu T, Kida Y, Kuwano K. 2011. Cytoadherence-dependent induction of inflammatory responses by *Mycoplasma pneumoniae*. Immunology 133:51–61. https://doi.org/10.1111/j.1365-2567.2011.03408.x.
16. Khare S, Dorfleutner A, Bryan NB, Yun C, Radian AD, de Almeida L, Rojanasakul Y, Stehlik C. 2012. An NLRP7-containing inflammasome mediates recognition of microbial lipopeptides in human macrophages. Immunity 36:464–476. https://doi.org/10.1016/j.immuni.2012.02.001.
17. Xu Y, Li H, Chen W, Yao X, Xing Y, Wang X, Zhong J, Meng G. 2013. *Mycoplasma hyorhinis* activates the NLRP3 inflammasome and promotes migration and invasion of gastric cancer cells. PLoS One 8:e77955. https://doi.org/10.1371/journal.pone.0077955.
18. Sugiyama M, Saeki A, Hasebe A, Kamesaki R, Yoshida Y, Kitagawa Y, Suzuki T, Shibata K. 2016. Activation of inflammasomes in dendritic cells and macrophages by *Mycoplasma salivarium*. Mol Oral Microbiol 31:259–269. https://doi.org/10.1111/omi.12117.
19. Goret J, Le Roy C, Touati A, Mesureur J, Renaudin H, Claverol S, Bébéar C, Beven L, Pereyre S. 2016. Surface lipoproteome of *Mycoplasma hominis* PG21 and differential expression after contact with human dendritic cells. Future Microbiol 11:179–194. https://doi.org/10.2217/fmb.15.130.
20. Pereyre S, Sirand-Pugnet P, Beven L, Charron A, Renaudin H, Barré A, Avenaud P, Jacob D, Couloux A, Barbe V, de Daruvar A, Blanchard A, Bébéar C. 2009. Life on arginine for *Mycoplasma hominis*: clues from its minimal genome and comparison with other human urogenital mycoplasmas. PLoS Genet 5:e1000677. https://doi.org/10.1371/journal.pgen.1000677.
21. Braun V, Rehn K. 1969. Chemical characterization, spatial distribution and function of a lipoprotein (murein-lipoprotein) of the *E. coli* cell wall. The specific effect of trypsin on the membrane structure. Eur J Biochem 10:426–438.
22. Bella J, Hindle KL, McEwan PA, Lovell SC. 2008. The leucine-rich repeat structure. Cell Mol Life Sci 65:2307–2333. https://doi.org/10.1007/s00018-008-8019-0.
23. Fujita M, Into T, Yasuda M, Okusawa T, Hamahira S, Kuroki Y, Eto A, Nisizawa T, Morita M, Shibata K. 2003. Involvement of leucine residues at positions 107, 112, and 115 in a leucine-rich repeat motif of human Toll-like receptor 2 in the recognition of diacylated lipoproteins and lipopeptides and *Staphylococcus aureus* peptidoglycans. J Immunol 171:3675–3683. https://doi.org/10.4049/jimmunol.171.7.3675.
24. Bessler WG, Cox M, Lex A, Suhr B, Wiesmuller KH, Jung G. 1985. Synthetic lipopeptide analogs of bacterial lipoprotein are potent polyclonal activators for murine B lymphocytes. J Immunol 135:1900–1905.
25. Akazawa T, Inoue N, Shime H, Kodama K, Matsumoto M, Seya T. 2010. Adjuvant engineering for cancer immunotherapy: development of a synthetic TLR2 ligand with increased cell adhesion. Cancer Sci 101:1596–1603. https://doi.org/10.1111/j.1349-7006.2010.01583.x.
26. Okusawa T, Fujita M, Nakamura J, Into T, Yasuda M, Yoshimura A, Hara Y, Hasebe A, Golenbock DT, Morita M, Kuroki Y, Ogawa T, Shibata K. 2004. Relationship between structures and biological activities of mycoplasmal diacylated lipopeptides and their recognition by Toll-like receptors 2 and 6. Infect Immun 72:1657–1665. https://doi.org/10.1128/IAI.72.3.1657-1665.2004.
27. Lin XY, Choi MS, Porter AG. 2000. Expression analysis of the human caspase-1 subfamily reveals specific regulation of the CASP5 gene by lipopolysaccharide and interferon-gamma. J Biol Chem 275:39920–39926. https://doi.org/10.1074/jbc.M007255200.
28. Martinon F, Burns K, Tschopp J. 2002. The inflammasome: a molecular platform triggering activation of inflammatory caspases and processing of proIL-beta. Mol Cell 10:417–426. https://doi.org/10.1016/S1097-2765(02)00599-3.
29. Gurung P, Li B, Subbarao Malireddi RK, Lamkanfi M, Geiger TL, Kanneganti TD. 2015. Chronic TLR stimulation controls NLRP3 inflammasome activation through IL-10 mediated regulation of NLRP3 expression and caspase-8 activation. Sci Rep 5:14488. https://doi.org/10.1038/srep14488.
30. Bose S, Segovia JA, Somarajan SR, Chang TH, Kannan TR, Baseman JB. 2014. ADP-ribosylation of NLRP3 by *Mycoplasma pneumoniae* CARDS toxin regulates inflammasome activity. mBio 5(6):302186–14. https://doi.org/10.1128/mBio.02186-14.
31. Mitsunari M, Yoshida S, Shoji T, Tsukihara S, Iwabe T, Harada T, Terakawa N. 2006. Macrophage-activating lipopeptide-2 induces cyclooxygenase-2 and prostaglandin E(2) via toll-like receptor 2 in human placental trophoblast cells. J Reprod Immunol 72:46–59. https://doi.org/10.1016/j.jri.2006.02.003.
32. Sokolowska M, Chen LY, Liu Y, Martinez-Anton A, Qi HY, Logun C, Alsaaty S, Park YH, Kastner DL, Chae JJ, Shelhamer JH. 2015. Prostaglandin E2 inhibits NLRP3 inflammasome activation through EP4 receptor and intracellular cyclic AMP in human macrophages. J Immunol 194:5472–5487. https://doi.org/10.4049/jimmunol.1401343.
33. Barré A, de Daruvar A, Blanchard A. 2004. MolliGen, a database dedicated to the comparative genomics of *Mollicutes*. Nucleic Acids Res 32(Database issue):D307–D310.
34. Zhang P, Dixon M, Zucchelli M, Hambiliki F, Levkov L, Hovatta O, Kere J. 2008. Expression analysis of the NLRP gene family suggests a role in human preimplantation development. PLoS One 3:e2755. https://doi.org/10.1371/journal.pone.0002755.
35. Hellemans J, Vandesompele J. 2011. qPCR data analysis—unlocking the secret to successful results, p 1–13. *In* Kennedy S, Oswald N (ed), PCR troubleshooting and optimization: the essential guide. Caister Academic Press, Poole, UK.
36. Shimizu T, Kida Y, Kuwano K. 2004. Lipid-associated membrane proteins of *Mycoplasma fermentans* and *M. penetrans* activate human immunodeficiency virus long-terminal repeats through Toll-like receptors. Immunology 113:121–129. https://doi.org/10.1111/j.1365-2567.2004.01937.x.
37. Asai Y, Makimura Y, Ogawa T. 2007. Toll-like receptor 2-mediated dendritic cell activation by a *Porphyromonas gingivalis* synthetic lipopeptide. J Med Microbiol 56:459–465. https://doi.org/10.1099/jmm.0.46991-0.
38. Oven I, Resman Rus K, Dusanic D, Bencina D, Keeler CL, Jr, Narat M. 2013. Diacylated lipopeptide from *Mycoplasma synoviae* mediates TLR15 induced innate immune responses. Vet Res 44:99. https://doi.org/10.1186/1297-9716-44-99.